THE JOURNAL OF BIOLOGICAL CHEMISTRY
Vol. 274, No. 41, Issue of October 8, pp. 29094–29101, 1999
Printed in U.S.A.

Interactions of Bismuth Complexes with Metallothionein(II)*

(Received for publication, June 7, 1999, and in revised form, July 20, 1999)

Hongzhe Sun‡, Hongyan Li‡, Ian Harvey§, and Peter J. Sadler‡¶

From the ‡Department of Chemistry, University of Edinburgh, Edinburgh EH9 3JJ and §Central Laboratory of the Research Councils Daresbury Laboratory, Warrington WA4 4AD, United Kingdom

Bismuth complexes are widely used as anti-ulcer drugs and can significantly reduce the side effects of platinum anti-cancer drugs. Bismuth is known to induce the synthesis of metallothionein (MT) in the kidney, but there are few chemical studies on the interactions of bismuth complexes with metallothionein. Here we show that Bi^{3+} binds strongly to metallothionein with a stoichiometry bismuth:MT = 7:1 (Bi_7MT) and can readily displace Zn^{2+} and Cd^{2+}. Bismuth is still bound to the protein even in strongly acidic solutions (pH 1). Reactions of bismuth citrate with MT are faster than those of $[Bi(EDTA)]^-$, and both exhibit biphasic kinetics. ^{1}H NMR data show that Zn^{2+} is displaced faster than Cd^{2+}, and that both Zn^{2+} and Cd^{2+} in the β-domain (three metal cluster) of MT are displaced by Bi^{3+} much faster than from the α-domain (four metal cluster). The extended x-ray absorption fine structure spectrum of Bi_7MT is very similar to that for the glutathione and *N*-acetyl-L-cysteine complexes $[Bi(GS)_3]$ and $[Bi(NAC)_3]$ with an inner coordination sphere of three sulfur atoms and average Bi–S distances of 2.55 Å. Some sites appear to contain additional short Bi–O bonds of 2.2 Å and longer Bi–S bonds of 3.1 Å. The Bi^{3+} sites in Bi_7MT are therefore highly distorted in comparison with those of Zn^{2+} and Cd^{2+}.

Metallothionein (MT)[1] is an intriguing, low molecular mass (~7 kDa), cysteine- and metal-rich protein. It was first isolated from equine renal cortex 40 years ago (1) and contains 61 amino acids, of which 20 are cysteine residues. Since then, similar proteins have been isolated from the kidney, liver, and intestines of a variety of animal species (2), fungi (3, 4), plants (5), and metal-resistant bacteria (6–8). The two major isoforms of mammalian MT (MT(I) and MT(II)) differ only in minor sequence changes and overall charge. Recently, the discovery of a growth inhibitory factor (GIF) from human brain tissue and nerve and its characterization as a metallothionein (MT-III) has stimulated new interests in studying this small protein (9, 10).

The functions of metallothionein are still not fully understood. It appears to play a fundamental role in the metabolism of copper and zinc ions under various physiological conditions (11, 12), including its ability to donate metal ions to apo-Zn^{2+} enzymes (13, 14). Metallothionein may also be important for sequestering toxic Cd^{2+} ions, and probably also Hg^{2+} (15), Au^+ (16, 17), and Pt^{2+} (18, 19), thereby preventing reactions with other cellular targets in mammals and other higher organisms (20). Metallothionein also appears to play a role in radical scavenging, stress response, and the pharmacology of metallodrugs and alkylating agents (12, 21, 22).

The best characterized mammalian metallothioneins contain a single polypeptide chain with seven bound metal ions (either Zn^{2+} or Cd^{2+}). The x-ray crystal structure of rat liver Zn_2Cd_5-MT(II) (23) and NMR solution structures of rabbit liver Cd_7-MT(II) (24), rat liver Cd_7-MT(II) (25), and human liver Cd_7-MT (26) show that metallothionein contains two structurally independent α (C-terminal) and β (N-terminal) domains, which are linked in the protein via two amino acids. The seven metal ions are present in clusters of four and three metals bound to bridging and terminal cysteine thiolate ligands, with metal-to-thiolate ratios of M_4S_{11} and M_3S_9 for the α- and β-domains, respectively (23). When both Zn^{2+} and Cd^{2+} are present, Cd^{2+} binds preferentially to the α-domain, whereas Zn^{2+} is found preferentially in the β-domain (23, 28). A Zn_2Cd three-metal cluster (β domain) in MT has the same structure as a Cd_3 cluster (23). The α-domain binds Cd^{2+} ions cooperatively (29). All 20-cysteine residues participate in metal binding, and each of the seven Zn^{2+} or Cd^{2+} ions is tetrahedrally coordinated to four cysteine thiolate sulfur atoms (30, 31).

Bismuth is known to induce the synthesis of renal metallothionein (32), and it has been shown that pretreatment with bismuth complexes can prevent the toxic side effects of the anti-cancer drug cisplatin without compromising its anti-tumor activity (33–36). The protection probably involves platinum binding to Bi-induced metallothionein. However, there are few chemical studies of the reaction of Bi^{3+} with metallothionein (37, 38). Such interactions could also play a crucial role in the pharmacology of widely used bismuth anti-ulcer drugs including colloidal bismuth subcitrate (De-Nol®) and ranitidine bismuth citrate (Pylorid® and Tritec®) (39–41). Here we report investigations of reactions of EDTA and citrate complexes of Bi^{3+} with metallothionein studied by UV, NMR, and x-ray absorption spectroscopy (XAS).

EXPERIMENTAL PROCEDURES

Materials—Rabbit liver Zn_7MT(II) (catalog number M9542) and Zn_2Cd_5MT(II) (catalog number M5392) were purchased from Sigma, and bismuth citrate [Bi(Hcit)] and ranitidine bismuth citrate (batch number 0018 E93K0441) were supplied by GlaxoWellcome plc. Bismuth citrate was dissolved in the minimum amount of ~10% ammonium hydroxide solution until it became a clear solution (pH ~7), and $[Bi(EDTA)]^-$, prepared according to the literature method (42), had a satisfactory elemental analysis. Solutions of $[Bi(EDTA)]^-$ were pre-

* This work was supported by GlaxoWellcome, the Engineering and Physical Sciences Research Council, Biotechnology and Biological Sciences Research Council, and the Committee of Vice-Chancellors and Principals (Overseas Research Student award to H. L.). The costs of publication of this article were defrayed in part by the payment of page charges. This article must therefore be hereby marked "*advertisement*" in accordance with 18 U.S.C. Section 1734 solely to indicate this fact.

¶ To whom correspondence should be addressed: Dept. of Chemistry, University of Edinburgh, King's Buildings, West Mains Rd., Edinburgh EH9 3JJ, UK. Tel.: 44-131-650-4729; Fax: 44-131-650-6452; E-mail: p.j.sadler@ed.ac.uk.

[1] The abbreviations used are: MT, metallothionein; H_4cit, citric acid; EXAFS, extended x-ray absorption fine structure; GSH, glutathione; NAC, *N*-acetyl-L-cysteine; pH*, pH meter reading in D_2O solution; XANES, x-ray absorption near edge structure; XAS, x-ray absorption spectroscopy; ICP-AES, inductively coupled plasma-atomic emission spectroscopy; TOCSY, total correlation spectroscopy; GIF, growth inhibitory factor.

pared by dissolving known amounts of solid $[Bi(EDTA)]^-$ in H_2O (or D_2O) and adjusting the pH to ~7.

Kinetics of Reactions of Bi^{3+} Complexes with $Zn_7MT(II)$—All the reactions were performed in 20 mM Tris-HCl buffer containing 10 mM NaCl at pH 7.4. Fresh solutions of metallothionein and bismuth complexes were purged for 10 min with argon or N_2 to prevent oxidation of the metallothionein. Concentrations of MT(II) were determined from the absorbance at 220 nm for $Zn_7MT(II)$ in 0.01 M HCl using $\Delta\epsilon$ = 47,300 M^{-1} cm^{-1} (43). To study reactions with Bi^{3+} complexes, 0.5 ml of $Zn_7MT(II)$ solution was placed into a 1-cm cuvette and sealed with parafilm. After temperature equilibration for ~10 min in the cuvette, 40 mol eq of Bi(III) complexes ($[Bi(cit)]^-$ or $[Bi(EDTA)]^-$) were added and the course of the reaction was monitored by UV spectrophotometry using a computer controlled Perkin-Elmer Lambda 16 spectrometer equipped with a PTP-1 temperature programmer. The absorbance recorded after 2 or 3 days was assumed to represent the equilibrium situation. The kinetic data were analyzed by a nonlinear least squares fitting based on an exponential function using the program Kaleidagraph (Synergy Software). Two kinetic steps were resolved which obeyed first-order kinetics.

Stoichiometry of Bismuth Metallothionein—Appropriate volumes of a 3.75 mM $[Bi(EDTA)]^-$ solution were added to 1.0-ml aliquots of 15 μM $Zn_7MT(II)$ (in 20 mM Tris-HCl, 10 mM NaCl, pH 7.4) to produce different molar ratios of $[Bi(EDTA)]^-$ to protein and the samples were left for about 1–2 days at 298 K to equilibrate. The absorbance at 350 nm (Bi–S ligand-to-metal-charge-transfer band) was recorded, and the stoichiometry of Bi-MT was obtained from the titration curve. The total sulfur content (due to cysteine and methionine), bismuth, cadmium, and zinc contents were also measured using the ICP-AES (Thermo Jarrell Ash, IRIS) at 180.731 nm (sulfur), 223.061 nm (bismuth), 213.856 nm (zinc) and 226.502 nm (cadmium). The Bi-MT sample for ICP-AES was prepared as follows. After addition of 40 mol eq of $[Bi(EDTA)]^-$ to $Zn_2Cd_5MT(II)$ solution (pH 7.6, 50 mM phosphate buffer) and equilibration for 48 h at 298 K, excess of Bi^{3+}, and displaced Zn^{2+} and Cd^{2+} were removed by ultrafiltration (Centricon 3, Amicon). The final solution was diluted with 2% HNO_3, and the metal and sulfur contents were measured without any digestion of the sample (44).

^1H NMR Studies of Reactions of Bi^{3+} with $Zn_2Cd_5MT(II)$ and $Zn_7MT(II)$—^1H NMR spectra of 0.5 mM rabbit liver $Zn_2Cd_5MT(II)$ or $Zn_7MT(II)$ (50 mM phosphate buffer, pH* 7.6) were recorded on a Bruker DMX500 spectrometer operating at 500.13 MHz at 298 K. Typical pulsing conditions for ^1H were: 7-μs pulse width, 16,384 data points, 3-s recycle delay, 16–64 transients. A two-dimensional TOCSY spectrum (mixing time 65 ms) was acquired using 2048 data points in f2 dimension, acquisition time 0.13 s, 48 scans, and 320 increments in the f1 dimension, in a total time of 14 h. All solutions were purged with nitrogen for at least 5 min. After recording an initial proton NMR spectrum, a 40-fold excess over protein of either $[Bi(EDTA)]^-$ or ranitidine bismuth citrate was added to the $Zn_2Cd_5MT(II)$ or $Zn_7MT(II)$ solution, and an NMR spectrum was recorded immediately (with ~3 min of mixing). Further spectra were recorded at frequent intervals over the next 9 h. Protein solutions were then allowed to react overnight, and small molecules were removed by ultrafiltration (Centricon 3) and washing four times with 50 mM deuterated phosphate buffer, each about 1.5 h, and then a two-dimensional TOCSY spectrum (mixing time 65 ms) was recorded. The peaks for $[Zn(EDTA)]^{2-}$ and $[Cd(EDTA)]^{2-}$ were integrated relative to the internal reference dioxane.

X-ray Absorption Spectroscopy Data Collection and Sample Preparation—X-ray spectra were recorded at the bismuth L_{III} edge on EXAFS station 7.1 at the Daresbury Laboratory Synchrotron Radiation Source. The operating energy was 2 GeV, and average current was approximately 200 mA. Powder samples were finely ground and mounted either as thin films or diluted appropriately with boron nitride. Solution samples were contained in sample cells with mylar windows and a 2-mm path length. In addition to the model compounds used for calibrating phase shifts, two model complexes $[Bi(GS)_3]$ and $[Bi(NAC)_3]$ were also studied by XAS for comparison. Data for the glutathione and *N*-acetyl-L-cysteine complexes were collected at ambient temperature in transmission mode using argon/helium-filled ionization chambers (up to three scans per sample). Data for the Bi_7MT samples were collected at 100 K in fluorescence mode using a scintillation detector (five to eight scans). The monochromator was detuned to 70% to reject harmonics. X-ray damage was checked by comparison of the data sets during collection and by the absence of color changes or edge shifts; there was no evidence of radiation damage to any samples. Samples were prepared as follows. For $[Bi(GS)_3]$ and $[Bi(NAC)_3]$, 3 mol eq of GSH or NAC were added to 50 mM $[Bi(cit)]^-$ followed by adjustment of the pH to ~7.0. Powder samples were prepared by freeze-drying the solution samples. For Bi_7MT, 5 mg of $Zn_2Cd_5MT(II)$ was dissolved in ~1 ml of 20 mM Tris-HCl buffer, pH 7.6, deoxygenated with N_2, and 40 mol eq of $[Bi(cit)]^-$ was added and equilibrated overnight. Some yellow participate appeared in this yellow solution and was separated by centrifugation, washed three times with water, and finally freeze-dried giving a slightly brown solid (hereafter called "brown MT precipitate"). The excess of $[Bi(cit)]^-$ was removed from the yellow solution by ultrafiltration three times using water as eluant (Centricon 3), and the final yellow solution was freeze-dried to give a yellow solid (hereafter called Bi_7-MT).

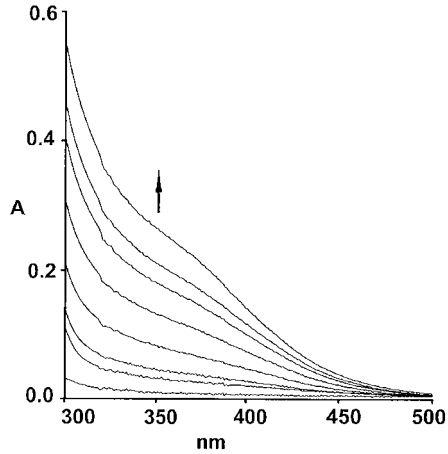

FIG. 1. **Displacement of Zn^{2+} from $Zn_7MT(II)$ by Bi^{3+}.** Dependence of absorption spectrum on time for a solution containing $Zn_7MT(II)$ (25 μM) and 40 mol eq of $[Bi(EDTA)]^-$ in 20 mM Tris-HCl, 10 mM NaCl buffer solution at pH 7.4, 298 K. The broad band centred at 350 nm is indicative of formation of Bi^{3+}–S (thiolate) bonds. Reaction times from *bottom* to *top*: 0, 2, 10, 30, 60, 90, 120, and 150 min.

X-ray Absorption Spectroscopy Data Analysis—Background subtraction was achieved using the motif-based SPLINE program (45, 65), modified for use with EXCURV. Data analysis was accomplished using EXCURV98 (46) via the single scattering curved-wave method for EXAFS calculations. Edge positions were calibrated against a Au foil at the L_{II} edge, taking the first derivative maximum as 13,734 eV. Phase shifts were derived from *ab initio* calculations within EXCURV98 and were extensively checked against the crystallographically characterized model compounds [Bi(HEDTA)], [{D-(−)-pencillaminato-*O, S,N*}BiCl] (47), $Na_2[Bi_2(citrate)_2]\cdot 7H_2O$ (48), $[Bi(SC_6F_5)_3(OPPh_3)_2]\cdot CH_2Cl_2$ and $[Bi(SC_6F_5)_3\{S{=}C(NHMe)_2\}_3]$ (49). Agreement between EXAFS and crystallographic parameters was better than ±0.01 Å for sulfur (±0.02 Å for 3–4 Å), ±0.02 Å for oxygen with sulfur present (±0.01 Å if no heavy scatterers present), and ±10% for coordination numbers. The EXAFS data were weighted by k^3 to compensate for the diminishing amplitude at high k. The data range used for analysis varied marginally between samples.

RESULTS

Kinetics of Reactions of Bismuth Complexes with $Zn_7MT(II)$—Reaction of bismuth complexes with rabbit liver $Zn_7MT(II)$ produced a new UV absorbance band centered at 350 nm. This was used to monitor the progress of reactions of bismuth complexes with metallothionein under pseudo first-order conditions (40-fold molar excess of Bi^{3+} over MT). Fig. 1 shows absorption spectra recorded for the reaction of excess $[Bi(EDTA)]^-$ with $Zn_7MT(II)$ at different times at 298 K, and the time course for the absorbance changes is shown in Fig. 2. The overall reaction was relatively slow, requiring over 10 h for completion. The reaction of $[Bi(cit)]^-$ with $Zn_7MT(II)$ gave rise to similar spectral changes, although it was much faster. About one-third of the total absorbance change occurred within the first 5 min. However, the total increase in absorbance for both reactions was similar after 1 or 2 days, indicating that equilibrium probably involved the formation of a similar final Bi-MT product.

Kinetic data were analyzed using the nonlinear least squares best fits based on an exponential function. The reaction of

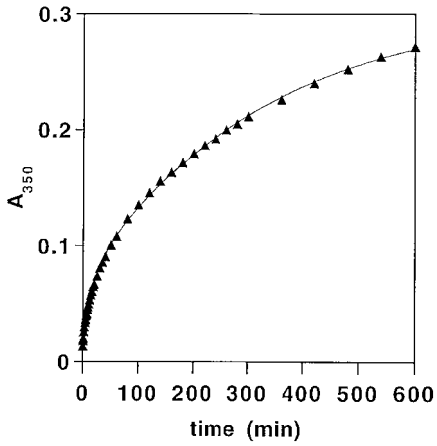

FIG. 2. **Determination of pseudo first-order rate constants for reaction of [Bi(EDTA)]$^-$ with Zn_7MT(II).** Dependence of absorbance at 350 nm on time for the reaction of [Bi(EDTA)]$^-$ (40 mol eq) with Zn_7MT(II) (25 μM) in 20 mM Tris-HCl, 10 mM NaCl, pH 7.4, 298 K. The curve is a nonlinear least squares fit using an exponential function.

[Bi(EDTA)]$^-$ and [Bi(cit)]$^-$ appeared to be biphasic; the rate constants are listed in Table I. The dependence of the rate on [Bi] was investigated for [Bi(cit)]$^-$. The first step appeared to be dependent of [Bi], Table I. The second step appeared to be independent of [Bi], and the rate was similar for [Bi(EDTA)]$^-$ and [Bi(cit)]$^-$.

Stoichiometry of Binding of Bi^{3+} to Metallothionein—The extent of bismuth binding to Zn_7MT was investigated in two ways: by determination of the change in absorption at 350 nm and by determination of the bismuth:sulfur ratio in the product via ICP-AES. Fig. 3 shows the change in the extinction coefficient at 350 nm ($\Delta\epsilon$) with variation of the [Bi(EDTA)]$^-$:Zn_7MT molar ratio. The value of $\Delta\epsilon$ increases linearly, and plateaus at a ratio of ~7.0, reaching a final value of ~15,000 M^{-1} cm^{-1}. By ICP-AES, the stoichiometry of purified Bi-MT (see "Experimental Procedures") was determined to be bismuth:sulfur = 1.0:3.0 ($\pm$0.1), and the mol ratio of bismuth:zinc > 170:1. Since there are 21 sulfur atoms in MT (20 Cys + 1 Met), the mol ratio of bismuth to MT is 7:1.

Effect of pH on Bi_7MT—A solution containing Bi_7MT was generated by reacting Zn_7MT (25 μM) with 40 mol eq of [Bi(EDTA)]$^-$ in 20 mM Tris-HCl buffer, 10 mM NaCl, pH 7.4, for about 1 day at 298 K, followed by ultrafiltration to remove excess [Bi(EDTA)]$^-$ and other low molecular mass molecules. With decreasing pH, the absorbance of Bi_7MT(II) at 350 nm decreased only slightly, and by <20% at pH values as low as 1.0, suggesting that Bi^{3+} remains bound to the protein even in strongly acidic solutions.

Gel Filtration Profile of Bi_7MT—Bi_7MT (prepared from Zn_7MT) exhibited a similar retention time to Zn_7MT when chromatographed on Superdex G-200.

^{1}H NMR Studies—Reactions of [Bi(EDTA)]$^-$ with Zn_7MT and Zn_2Cd_5MT(II) were followed by ^{1}H NMR spectroscopy. Since [Zn(EDTA)]$^{2-}$ and [Cd(EDTA)]$^{2-}$ formed via displacement of Zn^{2+} and Cd^{2+} from the protein have characteristic ^{1}H NMR shifts (50), it was possible to monitor the kinetics of displacement of these metal ions individually from the protein. The 500 MHz ^{1}H NMR spectra of rabbit liver Zn_2Cd_5MT(II) at different times after addition of 40 mol eq of [Bi(EDTA)]$^-$ are shown in Fig. 4. The intense resonances at ~3.1 ppm can be assigned largely to β protons of Cys and Lys residues, and the two singlets at 2.10 and 2.16 ppm to the *N*-acetyl-CH_3 and ϵCH_3, respectively, of the terminal *N*-acetylmethionine residue (51). The resonances at 0.8–1.7 ppm can be assigned to methyl groups of Ala, Ile, and Lys residues on the basis of their chemical shifts and coupling constants (51). The peaks that appear at 2.92, 2.76, and 2.65 ppm after addition of [Bi(EDTA)]$^-$ can be assigned to the ethylenic protons of EDTA complexed to [Zn(EDTA)]$^{2-}$, [Cd(EDTA)]$^{2-}$, and [Ca(EDTA)]$^{2-}$, respectively (50). Cadmium satellites (due to ^{111}Cd and ^{113}Cd, total natural abundance 25%) can be clearly observed for [Cd(EDTA)]$^{2-}$ peaks. The relative integrated areas of the peaks at 2.92 and 2.76 ppm (for [Zn(EDTA)]$^{2-}$ and [Cd(EDTA)]$^{2-}$, respectively), increased with time as shown in Fig. 5. Most of the Zn^{2+} was already present as an EDTA complex by the time the first spectrum was recorded (~3 min after addition of [Bi(EDTA]$^-$), whereas the peaks for [Cd(EDTA)]$^{2-}$ continued to increase in intensity for a period of about 6 h. There were no further changes to the spectrum after 15 h, at which point the relative integrated peak ratio [Zn(EDTA)]$^{2-}$:[Cd(EDTA)]$^{2-}$ at 2.92 and 2.76 ppm, was 2.0:5.3, which suggested that all Zn^{2+} and Cd^{2+} had been displaced from the protein by Bi^{3+}. Gradual changes were also observed for the metallothionein resonances during the course of the reaction. There was an overall broadening of the resonances, the peak at 1.16 ppm, which can be assigned to the β protons of Ala^{23} (CH_3) (24) disappeared, the intense peak at ~3.10 ppm decreased in intensity, and broadening of the two singlets at 2.10 and 2.16 ppm and peaks from 0.8–1.7 ppm was notable.

It can be seen clearly from Fig. 5 that Zn^{2+} was displaced from Zn_2Cd_5MT(II) by Bi^{3+} (added as [Bi(EDTA)]$^-$) very rapidly (within 3 min), while Cd^{2+} was displaced relatively slowly (>4 h). By the time the first spectrum was recorded, the [Cd(EDTA)]$^{2-}$ peak at 2.76 ppm had reached one-fifth of its final intensity (attained after overnight equilibration). After a further 5 min the peak had doubled in intensity. The rate constants for Cd^{2+} displacement were determined using nonlinear least squares best fits (Fig. 5). This was a biphasic process with pseudo first-order rate constants of 5.8×10^{-3} s^{-1} and 1.0×10^{-4} s^{-1} (half-lives of 2 min and 1.9 h, respectively), whereas the rate of Zn^{2+} displacement was too fast to determine accurately by NMR spectroscopy.

The reaction of [Bi(EDTA)]$^-$ with Zn_7MT(II) was also investigated by ^{1}H NMR spectroscopy. About three-seventh of the Zn^{2+} was displaced within 3 min of mixing, and the rate could not be determined by NMR. The remaining Zn^{2+} was displaced by Bi^{3+} in a biphasic process. Using nonlinear least squares best fits, rate constants of 7.2×10^{-3} s^{-1} and ~5.9×10^{-5} s^{-1} (half-lives of 1.6 min and 3.3 h, respectively) were determined.

Studies of the reaction of the anti-ulcer compound ranitidine bismuth citrate with metallothionein using UV and NMR spectroscopy were hampered by the strong UV absorption from ranitidine and intense ^{1}H NMR signals of ranitidine and citrate. However, yellow solutions were obtained when ranitidine bismuth citrate was added to metallothionein under conditions similar to those used for [Bi(EDTA)]$^-$ and [Bi(cit)]$^-$. The product obtained after ultrafiltration to remove excess ranitidine bismuth citrate and other small molecules was almost identical to Bi_7MT obtained from the reaction of [Bi(EDTA)]$^-$ with metallothionein as judged by ^{1}H NMR spectroscopy (data not shown).

The two-dimensional ^{1}H TOCSY NMR spectrum (mixing time 65 ms) of purified Bi_7MT is shown in Fig. 6 together with that for Zn_7MT for comparison. Notable is the absence of several cross peaks assignable to Cys β CH_2 protons (26, 52, 53) in the region 2.7–3.3 ppm for Bi_7MT (*boxed* in Fig. 6).

X-ray Spectroscopy—XANES and EXAFS measurements were made on solution and solid samples containing bismuth:glutathione and bismuth:*N*-acetyl-L-cysteine in molar ratios of 1:3 and on solid Bi-MT samples obtained by reacting excess [Bi(cit)]$^-$ with 0.7 mM Zn_2Cd_5MT(II).

TABLE I

Pseudo first-order rate constants for reactions of $Zn_7MT(II)$ and $Zn_2Cd_5MT(II)$ with $[Bi(EDTA)]^-$ and $[Bi(cit)]^-$

The conditions for UV reactions were 25 μM $Zn_7MT(II)$ in 20 mM Tris-HCl buffer containing 10 mM NaCl, pH 7.4, at 298 K, and for NMR, 0.5 mM proteins in 50 mM phosphate buffer, pH* 7.6, 298 K.

Bi complex	Concentration	Protein	$k_1 \times 10^3$ [a]	$k_2 \times 10^4$ [a]	Method
	mM		s^{-1}	s^{-1}	
$[Bi(EDTA)]^-$	1.02	$Zn_7MT(II)$	0.95 ± 0.2	0.5 ± 0.4	UV
	20	$Zn_7MT(II)$	7.2	0.59	NMR
	20	$Zn_2Cd_5MT(II)$	5.8	1.0	NMR
$[Bi(cit)]^-$	5.08	$Zn_7MT(II)$	5.3 ± 0.4	0.57 ± 0.7	UV
	2.54	$Zn_7MT(II)$	4.6 ± 0.2	1.2 ± 0.3	UV
	1.02	$Zn_7MT(II)$	4.0 ± 0.5	1.1 ± 0.4	UV
	0.51	$Zn_7MT(II)$	3.2 ± 0.5	1.0 ± 0.2	UV

[a] Average ± S.D. for two to three experiments for UV measurements.

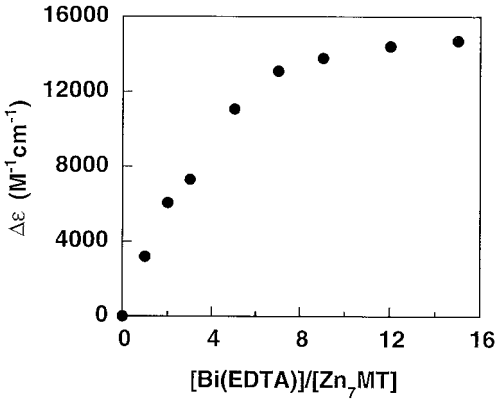

FIG. 3. **Stoichiometry of Bi^{3+} binding to Zn_7MT.** UV titration curve (350 nm) for addition of $[Bi(EDTA)]^-$ to $Zn_7MT(II)$ (15 μM) in 20 mM Tris-HCl containing 10 mM NaCl, pH 7.4. The overall absorbance changes suggest the formation of Bi_7MT (see text).

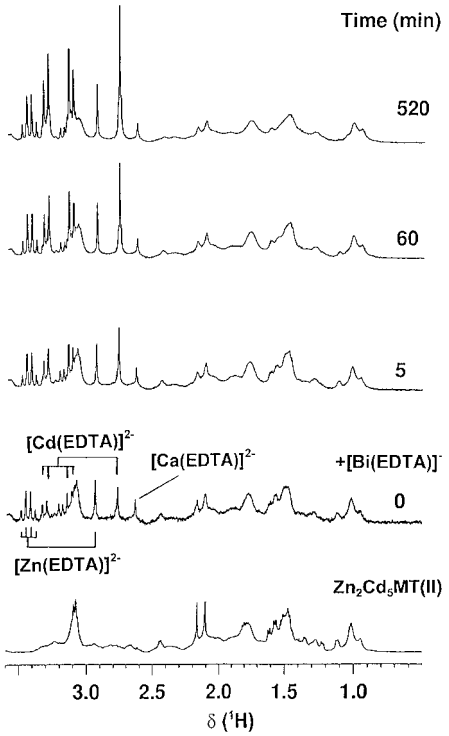

FIG. 4. **Displacement of Zn^{2+} and Cd^{2+} from $Zn_2Cd_5MT(II)$ by Bi^{3+}.** Dependence of the 500 MHz ^1H NMR spectrum of 0.5 mM $Zn_2Cd_5MT(II)$ (50 mM phosphate buffer, pH* 7.6, 298 K) on time after addition of 40 mol eq of $[Bi(EDTA)]^-$. The appearance of peaks for $[Zn(EDTA)]^{2-}$ and $[Cd(EDTA)]^{2-}$ is evident; the NCH_2 peaks appear as singlets and the $CH_2CO_2^-$ peaks as quartets (with $^{111,113}Cd$ satellites for $[Cd(EDTA)]^{2-}$). A small amount of Ca^{2+} (~0.5 Ca^{2+}/MTII) is also released by the protein and becomes bound to EDTA.

XANES spectra at the Bi L_{III} edge are broad and featureless due to the large core-hole lifetime (data not shown). However, there is a significant difference in the bismuth L_{III} edge positions between sulfur-containing and light-atom complexes of the order of 10 eV (13,425 eV for $[Bi(SC_6F_5)_3(OPPh_3)_2]\cdot CH_2Cl_2$ and $[Bi(SC_6F_5)_3\{S{=}C(NHMe)_2\}_3]$, 13,436 eV for [Bi(HEDTA)], 13,434 eV for $Na[Bi(citrate)]\cdot 7H_2O$. The edge positions for $[Bi(GSH)_3]$, $[Bi(NAC)_3]$, and both Bi-MT samples indicate that all these samples have sulfur-based ligation for bismuth.

The EXAFS data for $[Bi(GSH)_3]$ and $[Bi(NAC)_3]$ (both in solid and solution) are essentially identical. Analysis of the data (Table II and Fig. 7) gave rise to coordination numbers of 3.0 ± 0.3, with sulfur as the only coordinating atom, with an average Bi–S bond length of 2.56 Å.

The EXAFS spectra of the two Bi-MT samples (Bi_7-MT and brown MT precipitate) were quite distinct from each other. By comparing the EXAFS of Bi_7MT (Fig. 7ii) with those of $[Bi(GS)_3]$ (Fig. 7*A*, *i*) and $[Bi(NAC)_3]$, it can be seen that the coordination number of bismuth in Bi_7MT is similar to that of bismuth in $[Bi(GS)_3]$ and $[Bi(NAC)_3]$. The Fourier transform for Bi_7-MT is dominated by a single shell best simulated with 3.0 ± 0.1 sulfur at 2.55 ± 0.01 Å, a similar distance and coordination number as those determined for the model complexes. Fits were attempted with other sulfur coordination numbers, but on refinement the coordination number always returned to 3. The Fourier transform suggests that additional weakly scattering shells are present, including a small amount of oxygen (0.5 ± 0.3) at 2.18 ± 0.02 Å. The coordination number for this shell is poorly defined, but it is certainly less than unity. There is also reasonable evidence that the small peak in the Fourier transform at ~3 Å is due to additional sulfur scattering (1.9 sulfurs) at 3.09 ± 0.1 Å. The refined coordination number of 1.9 for this additional shell has a large uncertainty (±2) and is highly correlated with its own Debye-Waller factor. Therefore, this parameter must be treated with caution. This type of split sulfur ligation has a number of precedents, including the model compound $[Bi(SC_6F_5)_3\{S{=}C(NHMe)_2\}_3]$ used in this study (3 sulfurs at 2.72 Å, 3 sulfurs at 2.95 Å). X-ray fluorescence measurements on Bi_7MT gave bismuth: zinc > 17:1 (the very low level of zinc limited the measurement), in agreement with the ICP-AES measurement.

The brown MT precipitate sample gave much weaker EXAFS amplitudes compared with all the other samples. Fitting the data with a single shell of sulfurs resulted in large residuals in the Fit Index and the model was clearly incomplete in both the EXAFS and Fourier transform. Extensive analysis resulted in two different plausible models of equal quality. Both models suggest that the weaker EXAFS is due to destructive interference of two (or more) shells, rather than lower coordination numbers. Model 1 (Table II) consists of mixed oxygen (3.1 at 2.46 Å) and sulfur (4.1 at 2.51 Å) ligation. Model 2 is a split sulfur model (2.9 at 2.58 Å, 3.2 at 2.88 Å). Attempts to model

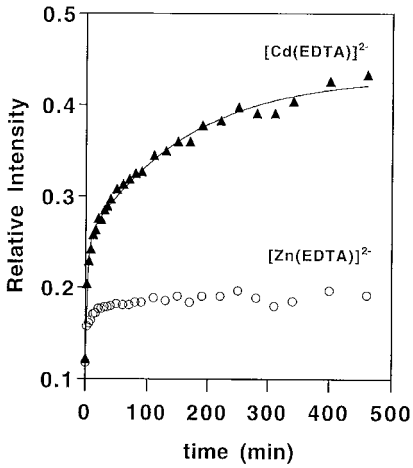

FIG. 5. **Kinetics of displacement of Zn^{2+} and Cd^{2+} by Bi^{3+}.** Dependence of relative areas of ^1H NMR peaks for zinc and cadmium EDTA on time for the reaction of 0.5 mM $Zn_2Cd_5MT(II)$ with 40 mol eq of $[Bi(EDTA)]^-$ at 298 K, in 50 mM phosphate buffer, pH* 7.6. Exponential fits give rate constants of $k_1 = 5.8 \times 10^{-3}$ s^{-1} and $k_2 = 1.0 \times 10^{-4}$ s^{-1} for the two phases of Cd^{2+} displacement.

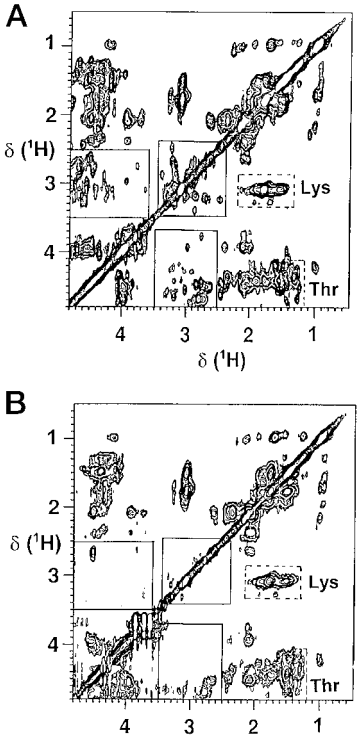

FIG. 6. **Two-dimensional TOCSY ^1H NMR spectra (mixing time 65 ms).** *A*, 0.5 mM rabbit liver $Zn_7MT(II)$; *B*, $Bi_7MT(II)$ in 50 mM phosphate buffer, pH* 7.6.

bismuth as a back-scatterer were unsuccessful. Although the models have equal fit indices, model 2 has a marginally lower R-factor (19.1% *versus* 20.3%). Additionally the difference in the Debye-Waller factors for the oxygen (0.004 $Å^2$) and sulfur (0.017 $Å^2$) in model 1 seems implausibly large. The refined coordination number for oxygen in model 1 is very highly correlated to a number of other parameters due the interference of the two scattering waves. Because of these potential problems with model 1 and the similarity of model 2 to known model systems, we suggest that model 2 is the more reliable. Brown MT precipitate may represent an intermediate (and less soluble) stage on the path to Bi_7-MT. It is not clear if it is a fully or partially loaded structural intermediate.

DISCUSSION

Metallothionein appears to play an important role in human health and disease as well as in the mechanism of action of therapeutic agents. Its synthesis is induced in biological systems by a variety of metal ions including Zn^{2+}, Cd^{2+}, Cu^+, and Bi^{3+}, and this induction may provide protection from toxicity by allowing sequestration of the metal (2). Metallothionein may also play a role in cellular resistance to Pt anti-cancer drugs (18, 19). Administration of bismuth can induce the synthesis of metallothionein in kidney but not in tumor tissue. This reduces the renal toxicity of cisplatin without compromising its chemotherapeutic activity (33, 36). Therefore it has been suggested that bismuth compounds are ideal for clinical application as adjuncts in chemotherapy with cisplatin. Bismuth compounds have been used in medicine for centuries, mainly for the treatment of peptic ulcers and gastric disorders. Therefore, MT may play an important role in the pharmacological activity of bismuth anti-ulcer drugs.

Metal ions have been reported to bind to MT with a variety of stoichiometries, ranging from 7, 10, to 12 and even up to 20 metal ions per protein molecule and with different geometries (from tetrahedral, square-planar, to linear). These include monovalent metal ions such as Au^+ (16) and Cu^+ (54, 55), divalent metal ions such as Zn^{2+}, Cd^{2+}, Co^{2+}, and Hg^{2+}, trivalent metal ions such as In^{3+} and Sb^{3+} (38), and TcO^{3+} (56, 57). In the present studies we determined the stoichiometry of Bi^{3+} binding to MT as 7:1 using both UV titration and ICP-AES to measure the metal and sulfur contents. This result is in agreement with previous brief reports (37, 38) on bismuth metallothionein. X-ray and NMR studies of $Zn_xCd_{7-x}MTs$ have shown that the metals are distributed in two clusters as M_4S_{11} (α) and M_3S_9 (β) with the metals coordinated tetrahedrally (30). Previously reported structural data are summarized in Table III. Surprisingly, our EXAFS data suggest that Bi^{3+} (ionic radius 1.03 Å) coordinates strongly to only three cysteine sulfurs with an average Bi–S bond length of 2.55 Å. This bond length is almost identical to that found in x-ray structures of low M_r Bi(III) thiolate complexes (Bi–S 2.5 to 2.6 Å) (49, 58). The fit for the EXAFS data for Bi_7MT suggests the presence of additional sulfur scattering at ~3.1 Å. To retain the metal clusters a much distorted tetrahedral geometry is required with three Bi–S bond distances of 2.55 Å and a longer Bi–S contact of ca. 3.1 Å. Although the 3.1 Å distance is well defined, the associated coordination number is not, and the required coordination number for distorted tetrahedral geometry is well within the error range. In the crystal structure of $[Bi(SC_6F_5)_3]$, Bi^{3+} coordinates to three sulfurs with Bi–S bond lengths of 2.53–2.58 Å, and an additional long Bi–S bond of 3.32 Å (49). Molecular modeling of Hg_7MT (59) suggests that the geometry of Hg^{2+} is distorted away from tetrahedral due to extensive interactions with solvent water. The recent EXAFS studies on Hg_7MT have shown that the nearest coordination number for Hg^{2+} is 2, with Hg–S bond lengths of 2.33 Å and two less well defined long bonds of ~3.4 Å (60). It has been thought that the binding site cage of MT is too small to accommodate the volume of tetrahedral HgS_4 units. However, Cd^{2+}, which has a similar ionic radius (0.92 Å) and the same charge, coordinates tetrahedrally to sulfurs of Cys residues. The coordination geometry is therefore largely dependent on the metal ion, *e.g.* Ag^+, digonal (CN, 2); Cu^+, trigonal (CN, 3) (61); and TcO^{3+}, square pyramidal (CN, 5) (57).

The presence of additional short Bi–O bonds (2.18 Å) for at least some of the Bi^{3+} ions in Bi_7MT suggests that some Bi^{3+} ions also have bound water, or more likely hydroxide or oxide, or possibly oxygen donors from amino acid side chains such as Ser, Thr, Asp, or Glu. Alkoxide donors from Ser or Thr are

TABLE II
EXAFS data

Bi^{3+} coordination number (*N*), Bi-ligand distances (*R*), Debye-Waller factors ($2\sigma^2$), fit index (*FI*), and R-factor (R). $R_{EXAFS} = \Sigma_i^N 1/\sigma_i(|\chi_i^{exp}(k) - \chi_i^{theor}(k)|) \times 100\%$.

Sample	*N*	*R*	$2\sigma^2$	*FI*	R
		Å	$Å^2$		%
$[Bi(GSH)_3]$ solution	3.1 sulfur	2.565	0.009	3.1	19.3
$[Bi(GSH)_3]$ powder	2.7 sulfur	2.553	0.012	7.1	28.6
$[Bi(NAC)_3]$ solution	2.8 sulfur	2.551	0.007	4.5	22.7
$[Bi(NAC)_3]$ powder	3.2 sulfur	2.571	0.010	3.8	22.6
Bi_7MT	3.0 sulfur	2.553	0.009	6.2	27.3
	1.9 ± 2.0 sulfur	3.092	0.039	5.6	24.0
	0.5 oxygen	2.180	0.001		
Brown MT ppt					
Model 1	2.9 sulfur	2.514	0.017	3.3	20.3
	2.10 oxygen	2.464	0.004		
Model 2	2.9 sulfur	2.576	0.014		
	3.2 sulfur	2.877	0.045	3.3	19.1

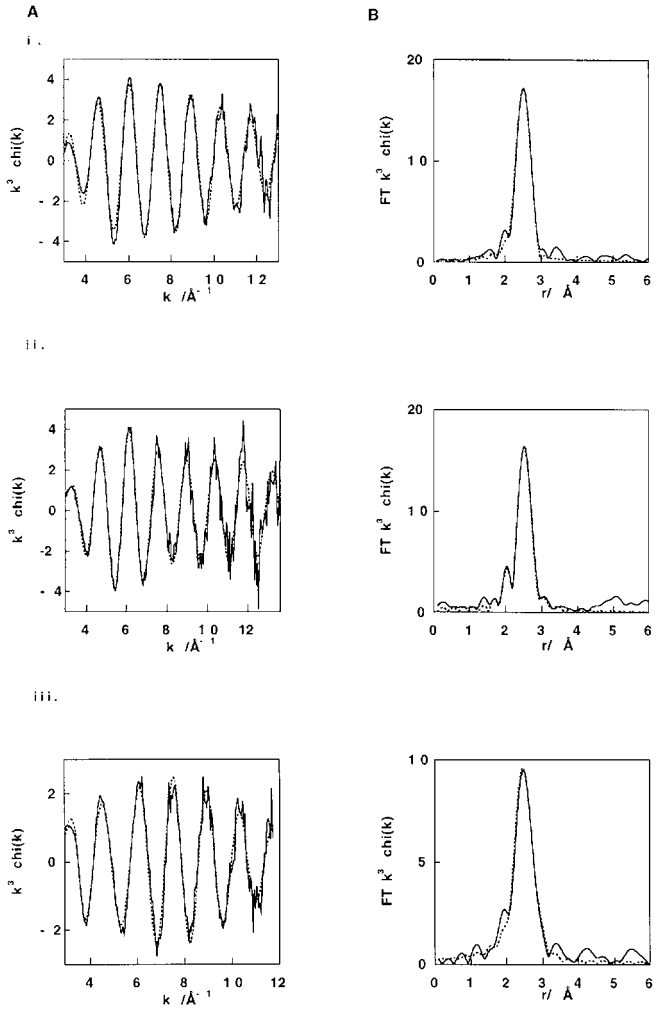

FIG. 7. **EXAFS spectra (*A*) and Fourier transforms (*B*) of the EXAFS spectra.** *i*, $[Bi(GS)_3]$ solution (*top*); *ii*, Bi_7MT (*middle*); *iii*, brown MT precipitate, model 2 (*bottom*). *Dotted line*, calculated; *solid line*, experimental.

attractive to consider because Bi–OR (alkoxide) bonds are known to be short and strong in several bismuth citrate adducts (41). No Ser or Thr side chains are particularly close to the metal clusters in zinc and cadmium metallothioneins with known structures, although Ser^{32} and Ser^{35} are less than 7 Å away from the M_4S_{11} cluster in the α domain, and Ser^2, Ser^{18}, and Ser^{28} are less than 7 Å from the M_3S_9 cluster in the β domain (23–25). Alkoxide coordination to Bi^{3+} often gives rise to lone-pair effects and distorted coordination spheres for Bi^{3+} (41). At biological pH, $Zn_xCd_yMT(II)$ ($x + y = 7$) is negatively charged (−2), whereas $Bi_7MT(II)$ would have an overall positive charge (+5). Thus the additional oxygen ligands may serve to neutralize the excess charge.

Previously we have shown (62) that Bi^{3+} binds to the Cys residue of glutathione and induces large low field shifts of the ^1H NMR resonances of β CH_2 protons (~1.4 ppm). Free and bismuth-bound glutathione exchange at an intermediate rate on the NMR time scale at biological pH (~1500 s^{-1}). The NMR data were also consistent with sulfur-only binding, in agreement with the EXAFS data. The overall broadening of the ^1H NMR spectrum of Bi_7MT and the disappearance of the two-dimensional TOCSY cross-peaks for β CH_2 of Cys residues (Fig. 6) suggest a facile exchange of Bi^{3+} between different sites, even though binding is thermodynamically very strong. Other cross-peaks, notably those for Lys and Thr, residues that are wide spread throughout the protein, remain unchanged in comparison with Zn_7MT, indicating that Bi_7MT probably has a folded conformation although the overall three-dimensional structure may be different. Our gel filtration chromatography studies show that Bi_7MT migrates in a similar manner to Zn_7MT, suggesting that their molecular masses and shapes are similar, *i.e.* Bi^{3+} has not induced MT polymerization. The disappearance of the β CH_3 ^1H NMR resonance of Ala^{23} (1.16 ppm) suggests that the structure of Bi_7MT in this region may be more flexible, and involved in dynamic exchange between different conformations. Previous molecular modeling studies have shown that Cys^{26} in the β domain is more solvent accessible and can be displaced from Zn^{2+} binding by the thiolate sulfur of glutathione (63).

Bi–S bonds in MT(II) appear to be remarkably stable even down to pH values near 1.0, in contrast to Zn^{2+} and Cd^{2+}, which are 50% dissociated at pH 4.6 and 3.05, respectively (55), but similar in strength to Cu^+-MT ($pH_{½}$ 0.44) (55). The affinity of Bi^{3+} for MT(II) is therefore higher than that of Zn^{2+} and Cd^{2+}.

The kinetics of reactions between bismuth complexes and MT(II) were elucidated in two ways: by observing the absorbance changes at 350 nm due to the formation of Bi–S bonds and the appearance of new ^1H NMR peaks resulting from the formation of either zinc or cadmium EDTA complexes after displacement of EDTA from Bi^{3+}. ^1H NMR also allowed the kinetics of Zn^{2+} and Cd^{2+} displacement by Bi^{3+} to be monitored separately. Biphasic processes were observed for both $[Bi(cit)]^-$ and $[Bi(EDTA)]^-$. In the fast step, the displacement of Zn^{2+} from Zn_7MT by $[Bi(cit)]^-$ occurred four times faster than that by $[Bi(EDTA)]^-$, while the second step was very similar for both of these bismuth complexes. This is probably due to differences

TABLE III
Summary of structural parameters for various metallothioneins (for references, see text)

Metal	Sample	Coordination number (*N*)	Distance	Geometry	Method
			Å		
Zn^{2+}	Zn_2Cd_5MTII	4 sulfur	2.296 ~ 2.476	Tetrahedral	X-ray
Cd^{2+}		4 sulfur	2.440 ~ 2.621	Tetrahedral	
Zn^{2+}	Zn_7MTII	4 sulfur	2.35 ± 0.01	Tetrahedral	EXAFS
Cd^{2+}	Cd_7MTII	4 sulfur	2.50 ± 0.02	Tetrahedral	EXAFS
Cu^{+}	Cu_{12}MTII	3 sulfur	2.25 ± 0.02	Trigonal	EXAFS
	Cu_4GIF(1–32)	2.9 sulfur	2.25 ± 0.02	Trigonal	EXAFS
	Cu_6GIF(1–32)	3.1 sulfur	2.24 ± 0.02	Trigonal	EXAFS
Ag^{+}	Ag_{12}MTII	2 sulfur	2.45 ± 0.02	Diagonal	EXAFS
	Ag_{17}MTII	2 sulfur	2.44 ± 0.02	Diagonal	EXAFS
TcO^{3+}	MTI	2 sulfur	2.31 ± 0.02	Square	EXAFS
		2 nitrogen/oxygen	2.02 ± 0.02	Pyramidal	
Hg^{2+}	Hg_7MTII	2 sulfur	2.33 ± 0.02	Disordered	EXAFS
		2 sulfur	3.4	Tetrahedral	
		3 sulfur	2.42 ± 0.02		EXAFS
	Hg_{18}MTII	2 sulfur	2.42 ± 0.03	Trigonal?	EXAFS
		0.6 chlorine	2.57 ± 0.03		
Bi^{3+}	Bi_7MTII	3 sulfur	2.55 ± 0.02		EXAFS
		2 sulfur	3.09 ± 0.02		
		0.5 oxygen	2.18 ± 0.02		
Bi^{3+}	Brown Bismuth MTII	2.9 sulfur	2.58		EXAFS
		3.2 sulfur	2.88		

in structure:bismuth citrate contains dimeric units $[Bi_2(cit)_2]^{2-}$ (48) in which the Bi^{3+} ion has apparent vacant coordination sites (perhaps occupied by the 6 s^2 lone pair of electrons) and therefore may be able to attack Cys sulfur of MT more readily than $[Bi(EDTA)]^-$ in which the EDTA ligand is wrapped around Bi^{3+} (42). By comparing the kinetics of reaction of $[Bi(EDTA)]^-$ with Zn_7MT and with Zn_2Cd_5MT (with Zn^{2+} in the β-domain), we have shown that metal ions in β-domain of the MT can be replaced preferentially, and cooperatively and rapidly (within minutes) by Bi^{3+}, and there is little difference between the reactivity of Zn_3 and Zn_2Cd β-domains. The first step maybe involve displacement of metal ions in the β-domain by Bi^{3+} and one metal ion in the α domain, as judged from NMR data, and the second step may involve displacement of the other metal ions in the α-domain. There have been several previous studies of metal and ligand displacement from Zn_7MT and Cd_7MT (18, 19), and multiphase processes have always been observed. Biphasic kinetics have usually been explained on the basis of formation and breakdown of intermediates (18, 19). However only a single kinetic step for metal displacement has been observed for reaction of EDTA with Cd^{2+} in the β-domain of Cd_7MT, and also one Cd^{2+} in the α domain can be extracted by EDTA more readily than the other Cd^{2+} ions (64). Our NMR data indicated the rapid removal of a small amount of Ca^{2+} from the protein (0.5 Ca^{2+} per MTII) during reaction with $[Bi(EDTA)]^-$. We assume that this is surface bound Ca^{2+} which has little effect on the cluster structures. Its presence has been observed previously (50).

The high stability of bismuth metallothionein suggests that it could play a significant role in the mechanism of action of bismuth-based drugs both in bacteria and in man. It may be an important species for bismuth transport from the liver to the kidney and be involved in bismuth storage in the kidney. In addition, the neurotoxicity of bismuth drugs (encephalopathy) could be related to the binding of Bi^{3+} to the brain-specific metallothionein(III), since the distribution of Bi^{3+} in mouse brain is very similar to that of Cu^+ and Ag^+ (27).

CONCLUSIONS

We have established that Bi^{3+} originating from bismuth citrate anti-ulcer compounds and from $[Bi(EDTA)]^-$ binds very strongly to MT(II) and readily displaces Zn^{2+} and Cd^{2+}. Despite its higher charge, Bi^{3+} also forms a 7:1 complex (Bi_7-MT), the same stoichiometry for binding as zinc and cadmium. EXAFS data show that on average each Bi^{3+} is coordinated strongly to only 3 cysteine sulfurs (at 2.55 Å) in contrast to Zn^{2+} and Cd^{2+}, which have clusters based on $M(Cys)_4$ centers. The presence of less well defined longer Bi–S contacts of 3.1 Å for some Bi^{3+} ions suggests that Bi_7-MT does contain clusters, although Bi-Bi contacts were not detectable. For at least some of the Bi^{3+} ions in Bi_7-MT, there is additional oxygen coordination as short Bi–O bonds of 2.2 Å. These could arise from bismuth-alkoxide linkages to Ser or Thr side chains or perhaps from oxide coordination. Remarkably, Bi^{3+} is still bound to MT, even at low pH values (*e.g.* pH 1), again in contrast to Zn^{2+} and Cd^{2+}. Displacement of Zn^{2+} and Cd^{2+} from the β-domain (M_3S_9) by Bi^{3+} was much faster than from the α-domain. These differences between the structure and reactivity of bismuth metallothionein compared with zinc metallothionein are likely to have implications for its biological properties. Since bismuth citrate complexes are widely used as anti-ulcer drugs, and pretreatment with bismuth compounds can protect against some of the toxic side effects of the anti-cancer drug cisplatin, further studies of bismuth metallothionein are warranted.

Acknowledgments—We are grateful to The Central Laboratory of the Research Councils for the provision of the x-ray spectroscopic facilities at Daresbury Laboratory, Dr. N. C. Norman (University of Bristol) for the gift of two bismuth complexes for EXAFS experiments, and to K. C. Cheung for assistance during XAS data collection.

REFERENCES

1. Margoshes, M., and Vallee, B. L. (1957) *J. Am. Chem. Soc.* **79,** 4813–4814
2. Nordberg, M., and Kojima, Y. (1979) in *Metallothionein* (Kägi, J. H. R., and Nordberg, M., eds) pp. 41–116, Birkhäuser Verlag, Basel, Switzerland
3. Prinz, R., and Weser, U. (1975) *Hoppe-Seyler's Z. Physiol. Chem.* **356,** 767–773
4. Lerch, K. (1980) *Nature* **284,** 368–370
5. Rauser, W. E., and Curvetto, N. R. (1980) *Nature* **287,** 563–564
6. Higham, D. P., Sadler, P. J., and Scawen, M. D. (1983) *Inorg. Chim. Acta* **79,** 140–141
7. Higham, D. P., Sadler, P. J., and Scawen, M. D. (1984) *Science* **225,** 1043–1046
8. Daniels, M. J., Turner-Cavet, J. S., Selkirk, R., Sun, H., Parkinson, J. A., Sadler, P. J., and Robinson, N. J. (1998) *J. Biol. Chem.* **273,** 22957–22961
9. Uchida, Y., Takio, K., Ihara, Y., and Tomonaga, M. (1991) *Neuron* **7,** 337–347
10. Uchida, Y. (1993) in *Metallothionein III, Biological Roles and Medical Implications* (Suzuki, K. T., Imura, N., and Kimura, M., eds) pp. 315–328, Birkhäuser Verlag, Basel, Switzerland
11. Richards, M. P. (1989) *J. Nutr.* **119,** 1062–1070
12. Karin, M. (1985) *Cell* **41,** 9–10
13. Li, T. Y., Kraker, A. J., Shaw, C. F., III, and Petering, D. H. (1980) *Proc. Natl. Acad. Sci. U. S. A.* **77,** 6334–6338
14. Jiang, L., Maret, W., and Vallee, B. L. (1998) *Proc. Natl. Acad. Sci. U. S. A.* **95,** 3483–3488

15. Morcillo, M. A., and Santamaria, J. (1996) *Biometals* **9**, 213–220
16. Saito, S., and Kurasaki, M. (1996) *Res. Commun. Mol. Pathol. Pharmacol.* **93,** 101–107
17. Shaw, C. F., III (1992) in *Metallothioneins-Synthesis, Structure and Properties of Metallothioneins, Phytochelatins and Metal-Thiolate Complexes* (Stillman, M. J., Shaw, C. F., III, and Suzuki, K. T., eds) pp. 144–185, VCH Publishers, Inc., New York
18. Pattanaik, A., Bachowski, G., Laib, J., Lemkuil, D., Shaw, C. F., III, Petering, D. H., Hitchcock, A., and Saryan, L. (1992) *J. Biol. Chem.* **267,** 16121–16128
19. Lemkuil, D. C., Nettesheim, D., Shaw, C. F., III, and Petering, D. H. (1994) *J. Biol. Chem.* **269**, 24792–24797
20. Hamer, D. (1986) *Annu. Rev. Biochem.* **55,** 913–951
21. Endresen, L., Bakka, A., and Rugstad, H. A. (1983) *Cancer Res.* **43,** 2918–2926
22. Thornalley, P. J., and Vašák, M. (1985) *Biochim. Biophys. Acta* **827,** 36–44
23. Robbins, A. H., McRee, D. E., Williamson, M., Collett, S. A., Xuong, N. H., Furey, W. F., Wang, B. C., and Stout, C. D. (1991) *J. Mol. Biol.* **221,** 1269–1293
24. Arseniev, A., Schultze, P., Wörgötter, E., Braun, W., Wagner, G., Vašák, M., Kägi, J. H. R., and Wüthrich, K. (1988) *J. Mol. Biol.* **201,** 637–657
25. Schultze, P., Wörgötter, E., Braun, W., Wagner, G., Vašák, M., Kägi, J. H. R., and Wüthrich, K. (1988) *J. Mol. Biol.* **203,** 251–268
26. Messerle, B. A., Schäffer, A., Vašák, M., Kägi, J. H. K., and Wüthrich, K. (1990) *J. Mol. Biol.* **214,** 765–779
27. Ross, J. F., Switzer, R. C., Poston, M. R., and Lawhorn, G. T. (1996) *Brain Res.* **725,** 137–154
28. Otvos, J. D., and Armitage, I. M. (1980) *Proc. Natl. Acad. Sci. U. S. A.* **77,** 7094–7098
29. Boulanger, Y., Armitage, I. M., Milklossy, K. A., and Winge, D. R. (1982) *J. Biol. Chem.* **257,** 13717–13719
30. Vašák, M., and Kägi, J. H. R. (1983) in *Metal Ions in Biological Systems* (Sigel, H., ed) Vol. 15, pp. 213–273, Marcel Dekker, Inc., New York
31. Vašák, M., and Kägi, J. H. R. (1981) *Proc. Natl. Acad. Sci. U. S. A.* **78,** 6709–6713
32. Disilvestro, R. A., Liu, J., and Klaassen, C. D. (1996) *Res. Commun. Mol. Pathol. Pharmacol.* **93,** 163–170
33. Naganuma, A., Satoh, M., and Imura, N. (1987) *Cancer Res.* **47,** 983–987
34. Satoh, M., Naganuma, A., and Imura, N. (1988) *Toxicology* **53,** 231–237
35. Boogaard, P. J., Slikkerveer, A., Nagelkerke, J. F., and Mulder, G. J. (1991) *Biochem. Pharmacol.* **41,** 369–375
36. Satoh, M., Aoki, Y., and Tohyama, C. (1997) *Cancer Chemother. Pharmacol.* **40,** 358–362
37. Bernhard, W., Good, M., Vašák, M., and Kägi, J. H. R. (1983) *Inorg. Chim. Acta* **79,** 154–155
38. Nielson, K. B., Atkin, C. L., and Winge, D. R. (1985) *J. Biol. Chem.* **260,** 5342–5350
39. Baxter, G. F. (1989) *Pharm. J.* **243**, 805–810
40. Baxter, G. F. (1992) *Chem. Brit.* **28,** 445–448
41. Sun, H., Li, H., and Sadler, P. J. (1997) *Chem. Ber./Recueil* **130,** 669–681
42. Summers, S. P., Abboud, K. A., Farrah, S. R., and Palenik, G. J. (1994) *Inorg. Chem.* **33,** 88–92
43. Li, T. Y., Minkel, D. T., Shaw, C. F., III, and Petering, D. H. (1981) *Biochem. J.* **19,** 441–446
44. Cols, N., Romero-Isart, N., Capdevila, M., Oliva, B., Gonzàlez-Duarte, P., Gonzàlez-Duarte, R., and Atrian, S. (1997) *J. Inorg. Biochem.* **61,** 157–166
45. Ellis, P. D. (1995) *Studies of Metalloproteins Using X-ray Absorption Spectroscopy and X-ray Diffraction*, University of Sydney, Australia
46. Binsted, N. (1998) *EXCURV 98: CCLRC Daresbury Laboratory Computer Program*, Central Laboratory of the Research Councils Daresbury Laboratory, Warrington, UK
47. Herrmann, W. A., Herdtweck, E., and Pajdla, L. (1993) *Chem. Ber.* **126,** 895–898
48. Barrie, P. J., Djuran, M. I., Mazid, M. A., McPartlin, M., Sadler, P. J., Scowen, I. J., and Sun, H. (1996) *J. Chem. Soc. Dalton Trans.* 2417–2422
49. Farrugia, L. J., Lawlor, F. J., and Norman, N. C. (1995) *J. Chem. Soc. Dalton Trans.* 1163–1171
50. Higham, D. P., Nicholson, J. K., Overnell, J., and Sadler, P. J. (1986) *Environ. Health Perspect.* **65,** 157–165
51. Neuhaus, D., Wagner, G., Vašák, M., Kägi, J. H. R., and Wüthrich, K. (1985) *Eur. J. Biochem.* **151,** 257–273
52. Neuhaus, D., Wagner, G., Vašák, M., Kägi, J. H. R., and Wüthrich, K. (1984) *Eur. J. Biochem.* **143,** 659–667
53. Messerle, B. A., Schäffer, A., Vašák, M., Kägi, J. H. R., and Wüthrich, K. (1992) *J. Mol. Biol.* **225,** 433–443
54. Anthony, P., Fowle, D. A., and Stillman, M. J. (1997) *J. Chem. Soc. Dalton Trans.* 977–984
55. Rupp, H., and Weser, U. (1978) *Biochim. Biophys. Acta* **533,** 209–226
56. Morelock, M. M., Cormier, T. A., and Tolman, G. L. (1988) *Inorg. Chem.* **27,** 3137–3140
57. Jones, W. B., Elgren, T. E., Morelock, M. M., Elder, R. C., and Wilcox, D. E. (1994) *Inorg. Chem.* **33,** 5571–5578
58. Atwood, D. A., Cowley, A. H., Hernandez, R. D., Jones, R. A., Rand, L. L., Bott, S. G., and Atwood, J. L. (1993) *Inorg. Chem.* **32,** 2972–2974
59. Fowle, D. A., and Stillman, M. J. (1997) *J. Biomol. Struct. Dyn.* **14,** 393–406
60. Jiang, D. T., Heald, S. M., Sham, T. K., and Stillman, M. J. (1994) *J. Am. Chem. Soc.* **116,** 11004–11013
61. Gui, Z., Green, A. R., Kasrai, M., Bancroft, G. M., and Stillman, M. J. (1996) *Inorg. Chem.* **35,** 6520–6529
62. Sadler, P. J., Sun, H., and Li, H. (1996) *Chem. Eur. J.* **2,** 701–708
63. Brouwer, M., Brouwer, T. H., and Cashon, R. E. (1993) *Biochem. J.* **294,** 219–225
64. Gan, T., Munoz, A., Shaw, C. F., III, and Petering, D. H. (1995) *J. Biol. Chem.* **270,** 5339–5345
65. Ellis, P. D. (1996) XFIT for Windows '95, Australian Synchrotron Research Program, Sydney, Australia